Supplementary Material for structures 1, 3, 7 (DFT calculations)

Title:

EFFECT OF THE TRIMETHYLSILYL SUBSTITUENT ON REACTIVITY OF PERMETHYLTITANOCENE

Authors:

Jiří Pinkas, Lenka Lukešová, Róbert Gyepes, Ivana Císařová, Peter Lönnecke, Jiří Kubišta, Michal Horáček, Karel Mach

Contents:

Gaussian 98 reference; Gaussian 03 reference

Gaussian 98, Revision A.7,
M. J. Frisch, G. W. Trucks, H. B. Schlegel, G. E. Scuseria,
M. A. Robb, J. R. Cheeseman, V. G. Zakrzewski, J. A. Montgomery, Jr.,
R. E. Stratmann, J. C. Burant, S. Dapprich, J. M. Millam,
A. D. Daniels, K. N. Kudin, M. C. Strain, O. Farkas, J. Tomasi,
V. Barone, M. Cossi, R. Cammi, B. Mennucci, C. Pomelli, C. Adamo,
S. Clifford, J. Ochterski, G. A. Petersson, P. Y. Ayala, Q. Cui,
K. Morokuma, D. K. Malick, A. D. Rabuck, K. Raghavachari,
J. B. Foresman, J. Cioslowski, J. V. Ortiz, A. G. Baboul,
B. B. Stefanov, G. Liu, A. Liashenko, P. Piskorz, I. Komaromi,
R. Gomperts, R. L. Martin, D. J. Fox, T. Keith, M. A. Al-Laham,
C. Y. Peng, A. Nanayakkara, C. Gonzalez, M. Challacombe,
P. M. W. Gill, B. Johnson, W. Chen, M. W. Wong, J. L. Andres,
C. Gonzalez, M. Head-Gordon, E. S. Replogle, and J. A. Pople,
Gaussian, Inc., Pittsburgh PA, 1998.

Gaussian 03, Revision C.02,
M. J. Frisch, G. W. Trucks, H. B. Schlegel, G. E. Scuseria,
M. A. Robb, J. R. Cheeseman, J. A. Montgomery, Jr., T. Vreven,
K. N. Kudin, J. C. Burant, J. M. Millam, S. S. Iyengar, J. Tomasi,
V. Barone, B. Mennucci, M. Cossi, G. Scalmani, N. Rega,
G. A. Petersson, H. Nakatsuji, M. Hada, M. Ehara, K. Toyota,
R. Fukuda, J. Hasegawa, M. Ishida, T. Nakajima, Y. Honda, O. Kitao,
H. Nakai, M. Klene, X. Li, J. E. Knox, H. P. Hratchian, J. B. Cross,
C. Adamo, J. Jaramillo, R. Gomperts, R. E. Stratmann, O. Yazyev,
A. J. Austin, R. Cammi, C. Pomelli, J. W. Ochterski, P. Y. Ayala,
K. Morokuma, G. A. Voth, P. Salvador, J. J. Dannenberg,
V. G. Zakrzewski, S. Dapprich, A. D. Daniels, M. C. Strain,
O. Farkas, D. K. Malick, A. D. Rabuck, K. Raghavachari,
J. B. Foresman, J. V. Ortiz, Q. Cui, A. G. Baboul, S. Clifford,
J. Cioslowski, B. B. Stefanov, G. Liu, A. Liashenko, P. Piskorz,
I. Komaromi, R. L. Martin, D. J. Fox, T. Keith, M. A. Al-Laham,
C. Y. Peng, A. Nanayakkara, M. Challacombe, P. M. W. Gill,
B. Johnson, W. Chen, M. W. Wong, C. Gonzalez, and J. A. Pople,
Gaussian, Inc., Wallingford CT, 2004.

List of orbital energies for **1** and calculated UV-Vis spectrum for **1**

List of orbital energies for **1** using Gaussian 03, Revision C.02.
Time-dependant DFT using spin-unrestricted BPW91/6-311+G(3d,p); Douglas-Kroll-Hess 2nd order scalar relativistic calculation;
the geometry was the solid state structure optimized using unrestricted BPW91/6-311G(d,p)and an analytically computed Hessian.
Both calculations used a pruned integration grid consisting of 99 radial shells each having 590 angular points.

Orbitals 118 and 119 are singly occupied (there are 119 alpha and 117 beta electrons).
Orbitals 1-117 are doubly, 118 and 119 are singly occupied, the others are virtual.

Orbital energies for **1** (in atomic units):

Orb.	Alpha energy	Beta energy
112	-0.25609	-0.25579
113	-0.25512	-0.25483
114	-0.20153	-0.19644
115	-0.20120	-0.19555
116	-0.18708	-0.18218
117	-0.18036	-0.17713
118	-0.11642	-0.07396
119	-0.10667	-0.05804
120	-0.09431	-0.04807
121	-0.01946	-0.01575
122	-0.00705	-0.00647
123	-0.00653	-0.00546
124	-0.00366	-0.00330
125	-0.00364	0.00758
126	-0.00217	0.00854
127	0.00684	0.01204
128	0.00927	0.01340

Calculated UV-Vis spectrum for **1**:

State	Trans. energy	Oscillator strength	Orbital transition	Expansion coefficient
1	4921.52 nm	0.0000	118A -> 120A	1.54499
2	3887.25 nm	0.0000	119A -> 120A	1.02673
3	540.46 nm	0.0066	117A -> 120A	0.96284
			117B -> 118B	-0.33320
4	516.95 nm	0.0000	119A -> 121A	0.99075
5	493.79 nm	0.0032	116A -> 120A	0.98318
			116B -> 118B	-0.20547
6	470.36 nm	0.0000	118A -> 121A	0.99648

orbital 114

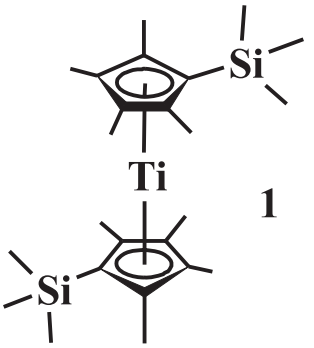

1

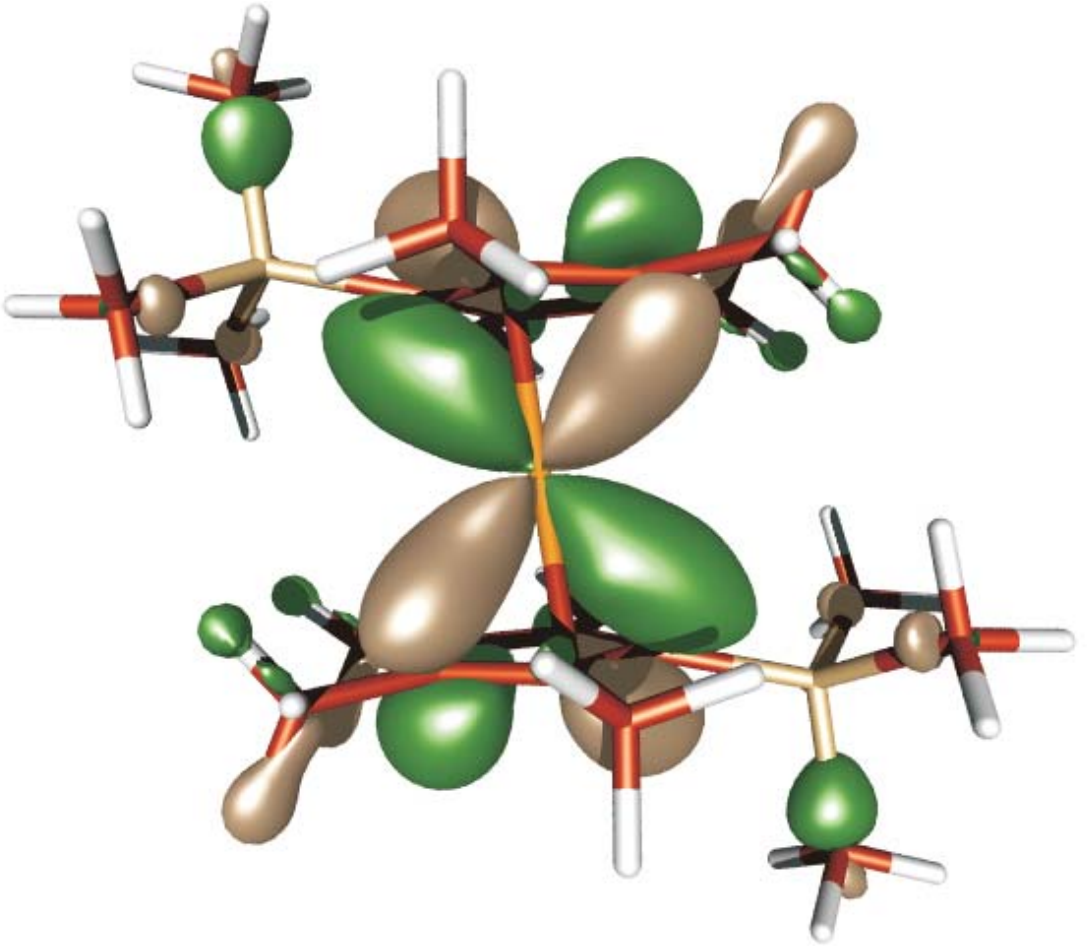

orbital 115

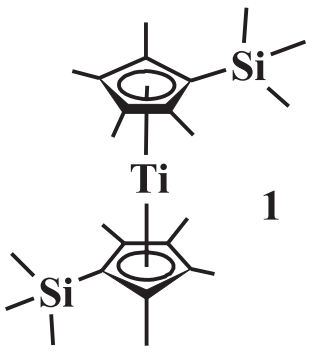

1

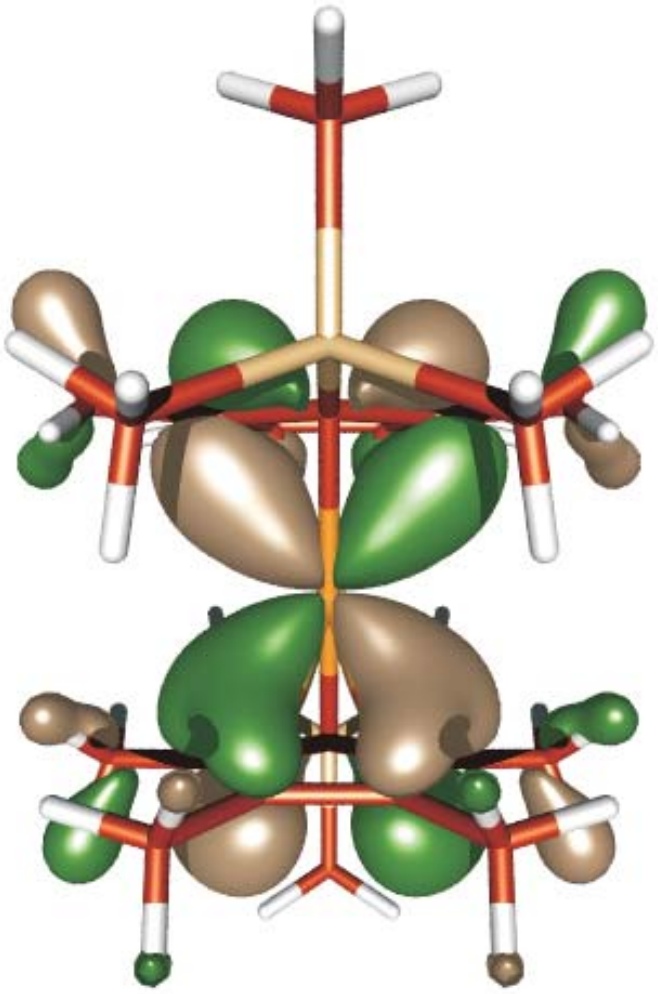

orbital 116

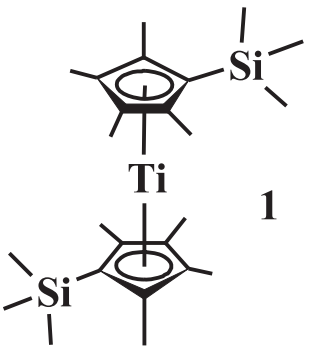

1

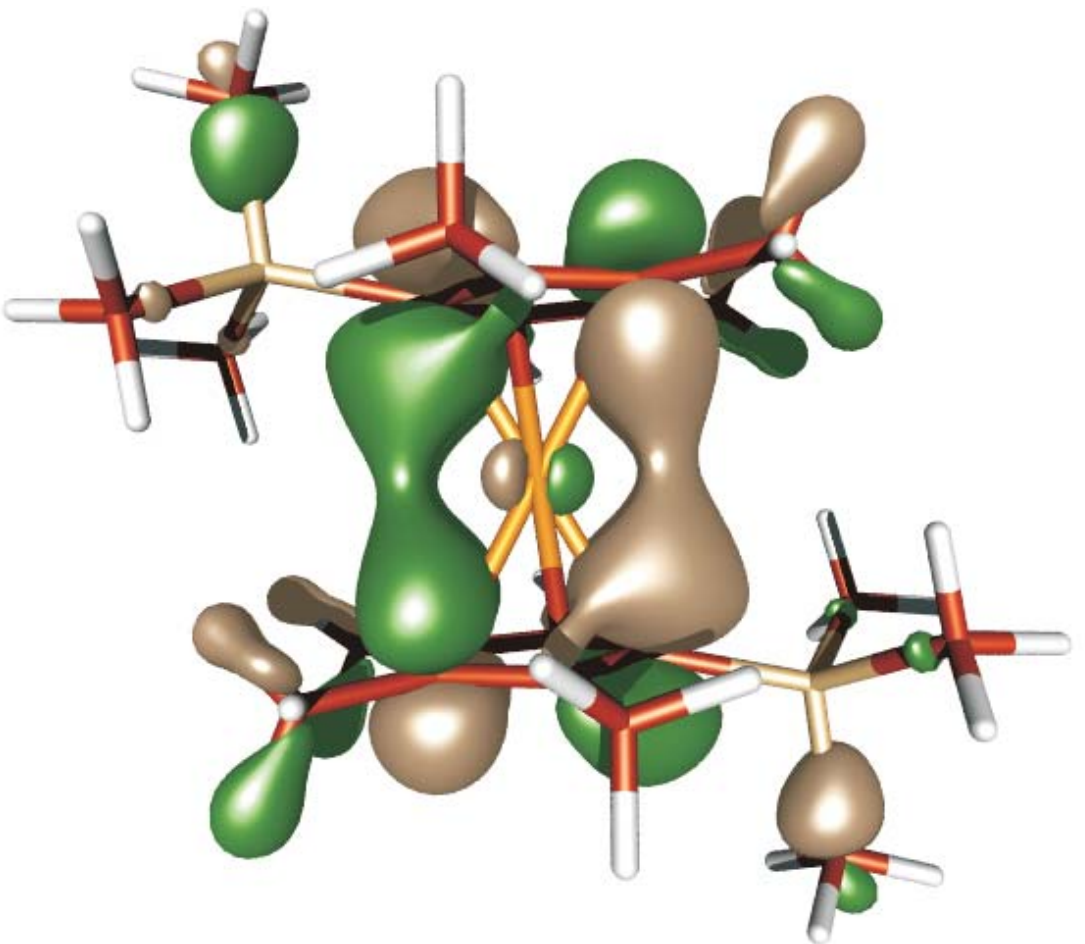

orbital 117

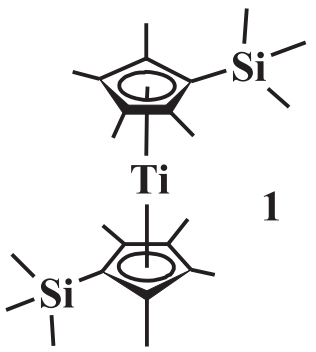

1

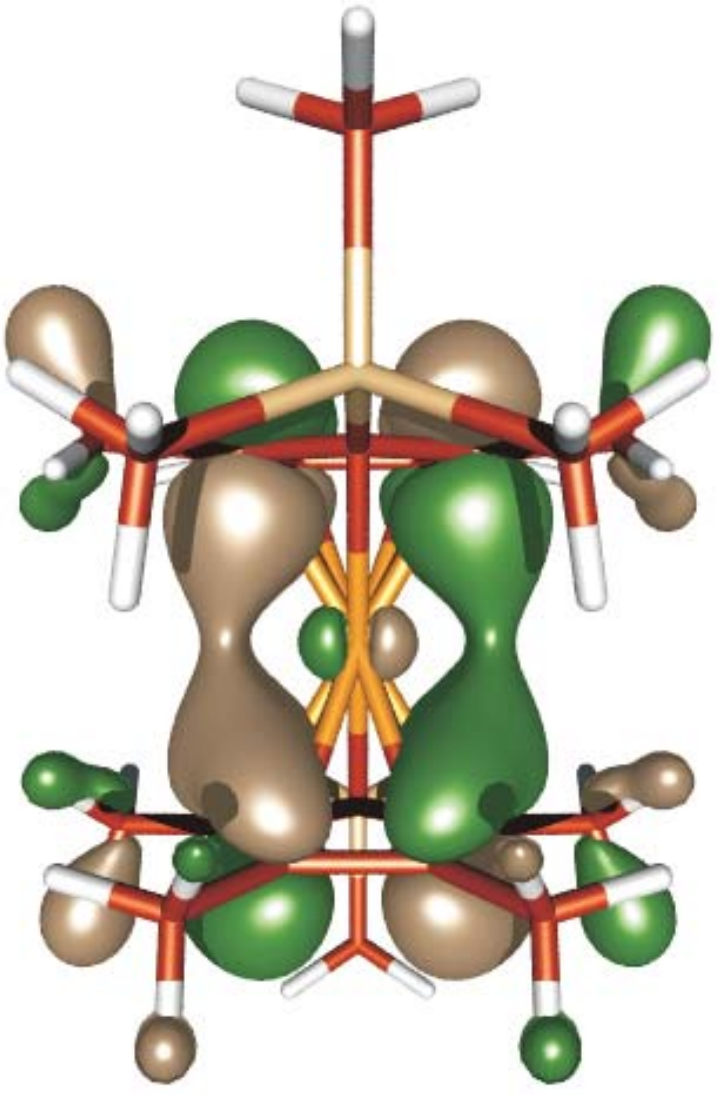

orbital 118

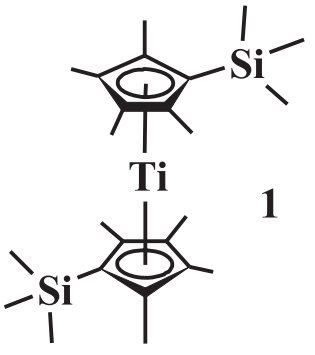

1

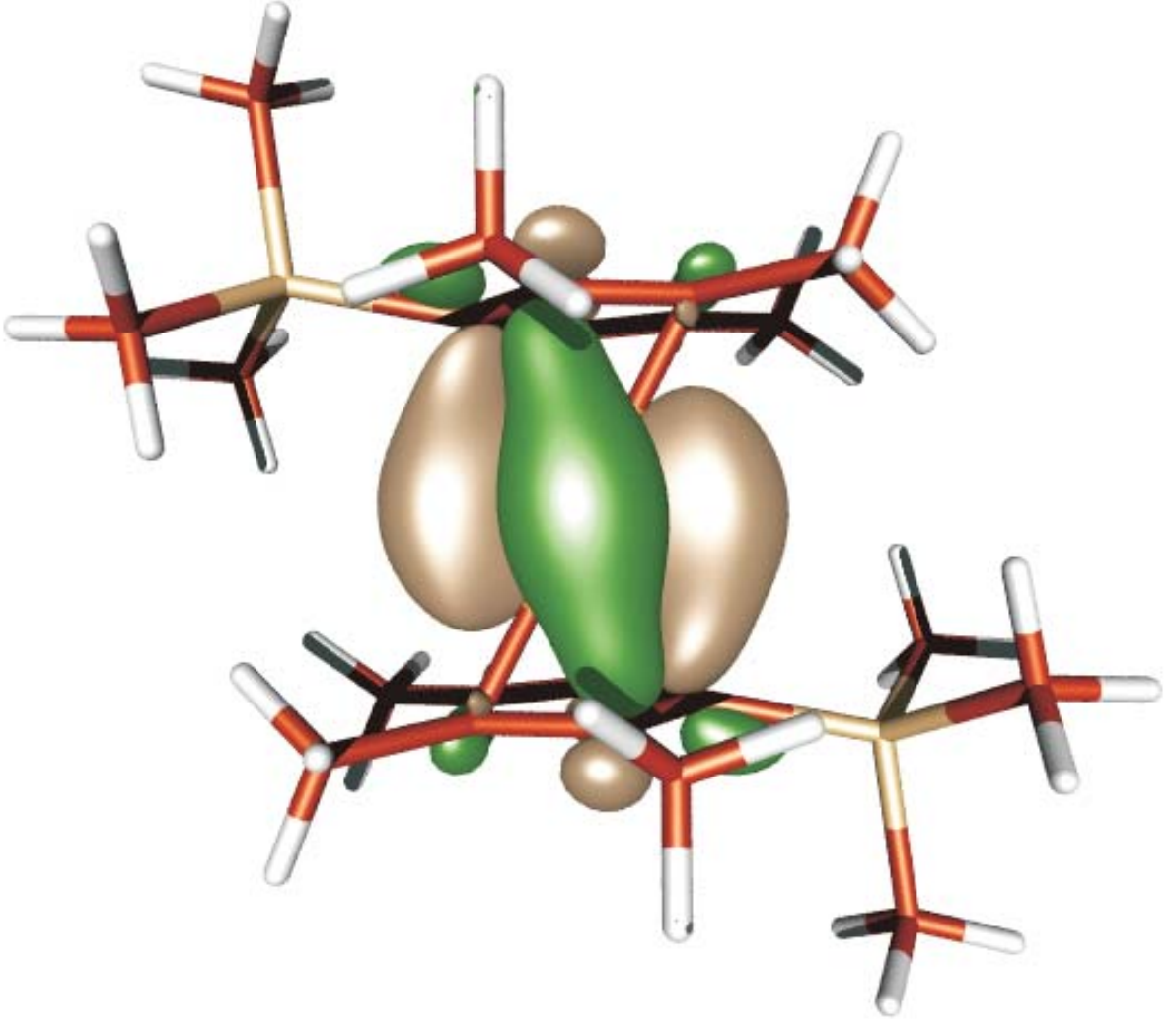

orbital 119

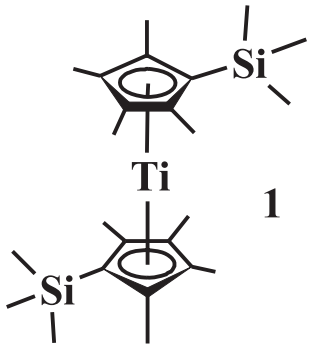

1

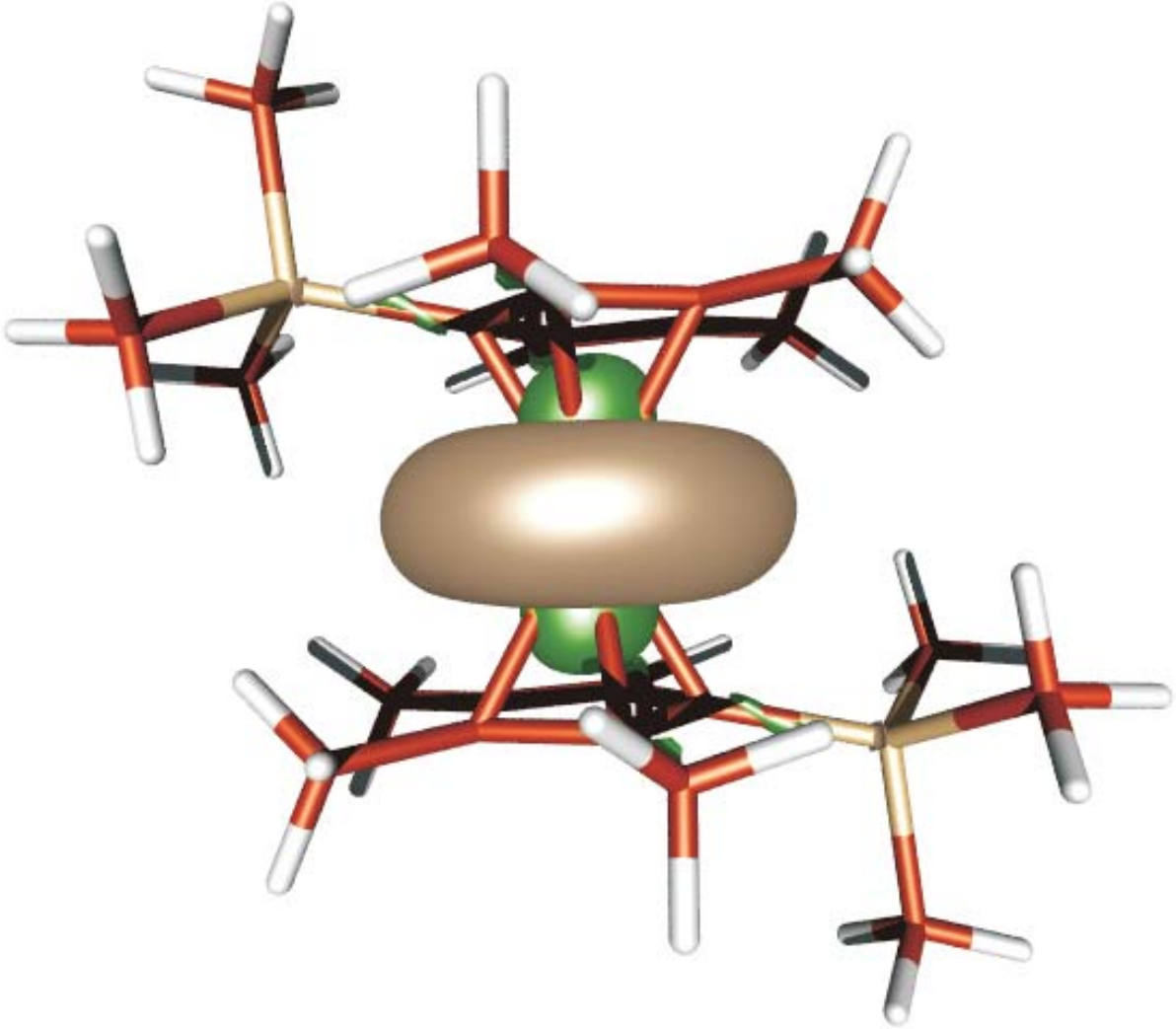

orbital 120

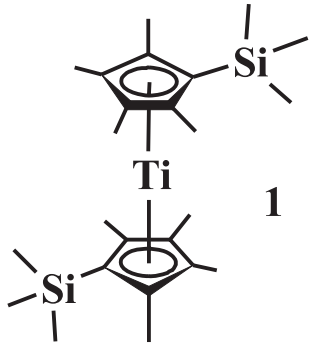

1

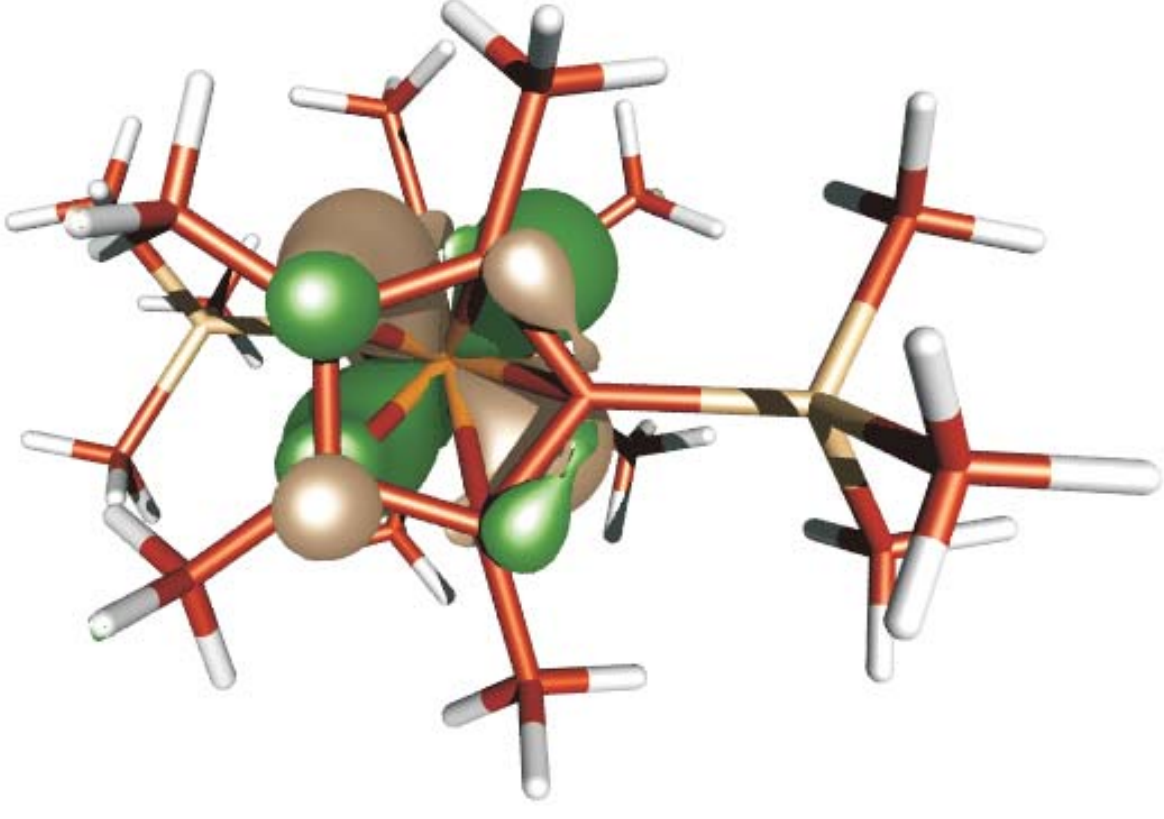

orbital 123

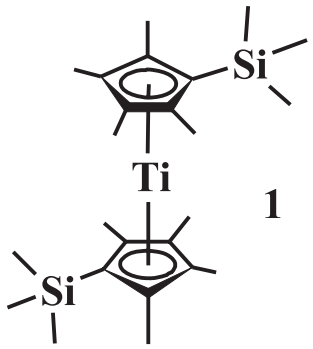

1

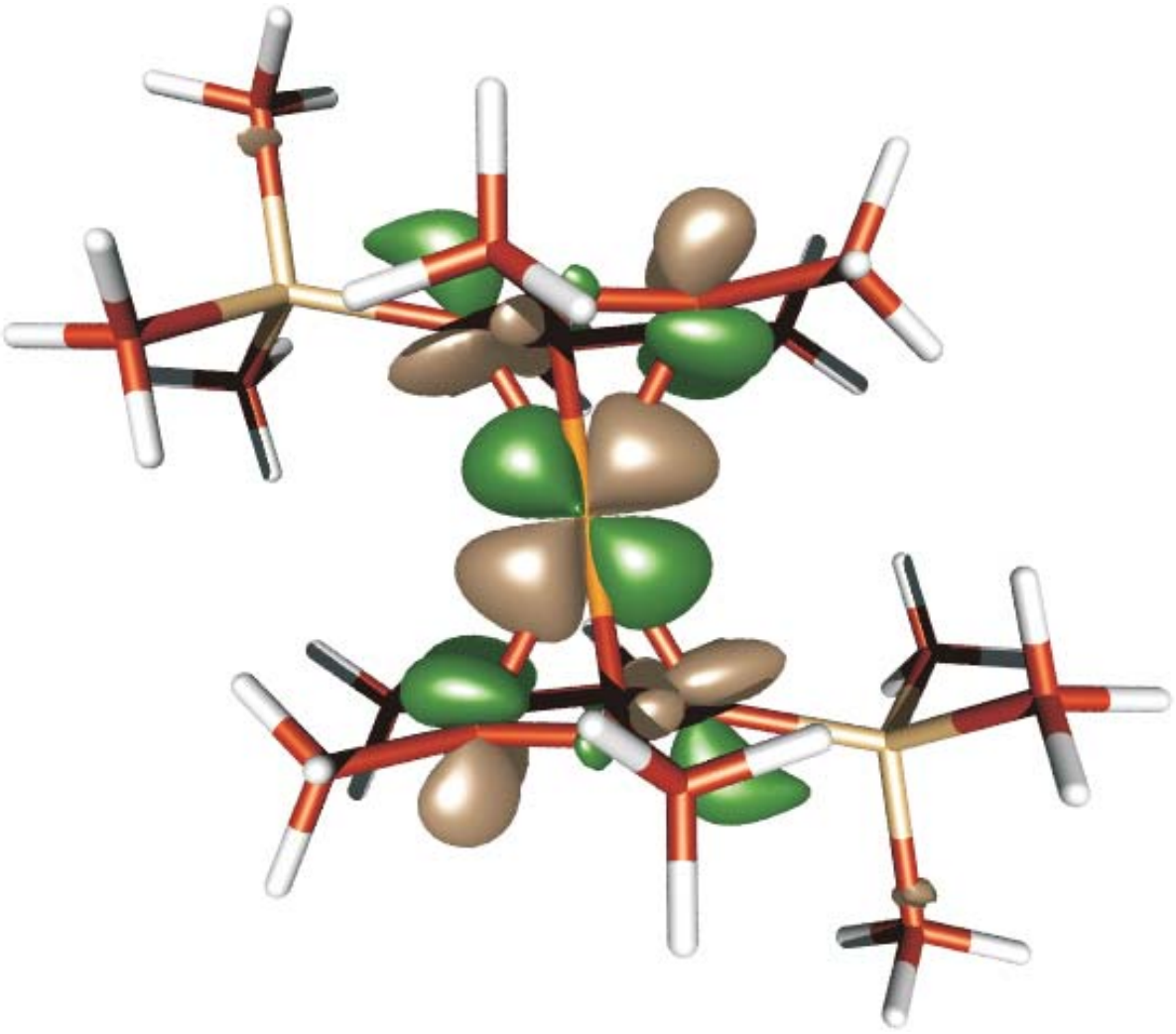

orbital 126

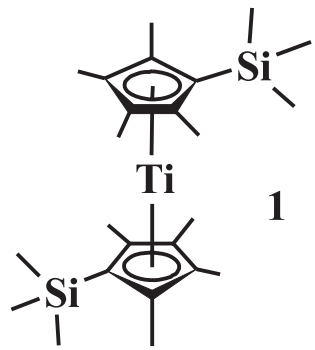

1

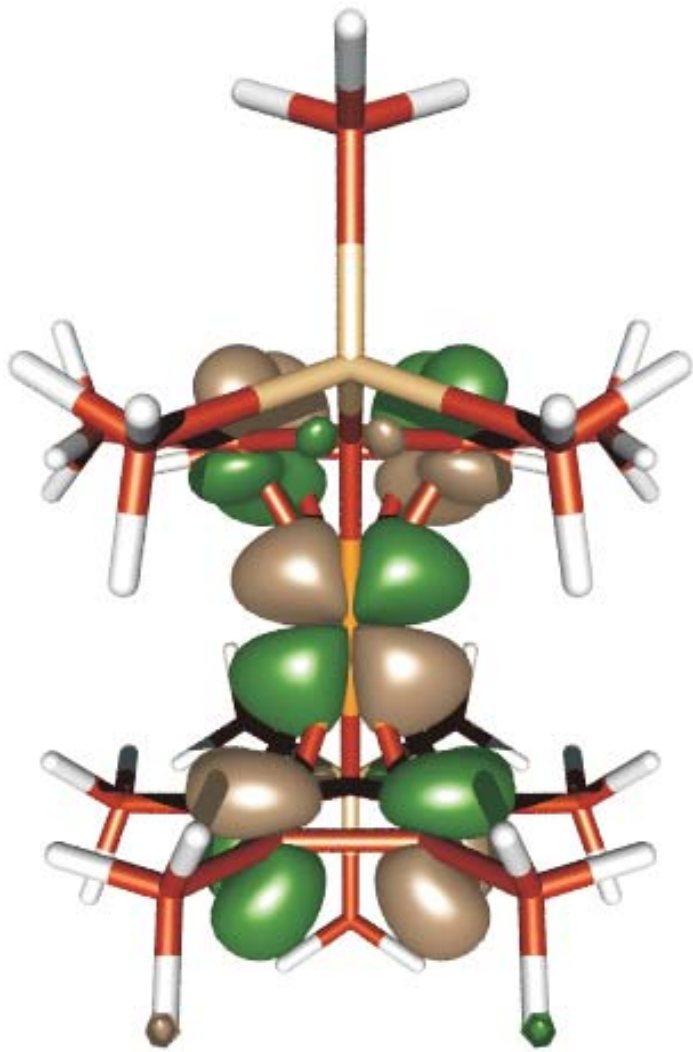

List of orbital energies for **3**.

Orbital energies for **3** (in atomic units).

Orb.	Energy	
100	-0.33414	
101	-0.30202	
102	-0.30086	
103	-0.29757	
104	-0.29202	
105	-0.29056	
106	**-0.28585**	**drawn at 7% probability level**
107	**-0.27115**	**drawn at 7% probability level**
108	**-0.26865**	**drawn at 7% probability level**
109	**-0.22509**	**drawn at 7% probability level**
110	**-0.22042**	**drawn at 7% probability level**
111	**-0.20596**	**drawn at 7% probability level**
112	**-0.18258**	**drawn at 7% probability level**
113	**-0.06387**	**drawn at 7% probability level**
114	**-0.02002**	**drawn at 7% probability level**
115	**0.00602**	**drawn at 7% probability level**
116	**0.01386**	**drawn at 7% probability level**
117	**0.02462**	**drawn at 7% probability level**
118	0.03241	
119	0.04299	
120	0.04853	
121	0.05222	
122	0.06046	

Calculated UV-Vis spectrum for **3**.

UV-Vis spectra of **3** obtained by time-dependant DFT: B3LYP/6-311G(2d) basis set on all atoms except the titanium, which employed the ECP by Hurley et al. Douglas-Kroll-Hess 2nd order scalar relativistic calculation; the geometry was the solid state structure optimized using BPW91/6-311G(d,p) and an estimated Hessian.
Both calculations used a pruned integration grid consisting of 99 radial shells each having 590 angular points.

UV-Vis spectra: the peak observed in UV-Vis spectra is actually a superposition of two overlapping peaks. According to time-dependent DFT results, the HOMO->LUMO transition lying at 746.92 nm has $\Delta l=2$, which is however not completely forbidden due to the presence of the metal. The transition between orbitals no. 111 -> no. 113 has $\Delta l=1$, having a calculated position at 587.94 nm. The decomposition of the experimental peak into two Gaussian peaks yielded the mean values 676.46±7.32 nm and 575.61±1.73 nm.

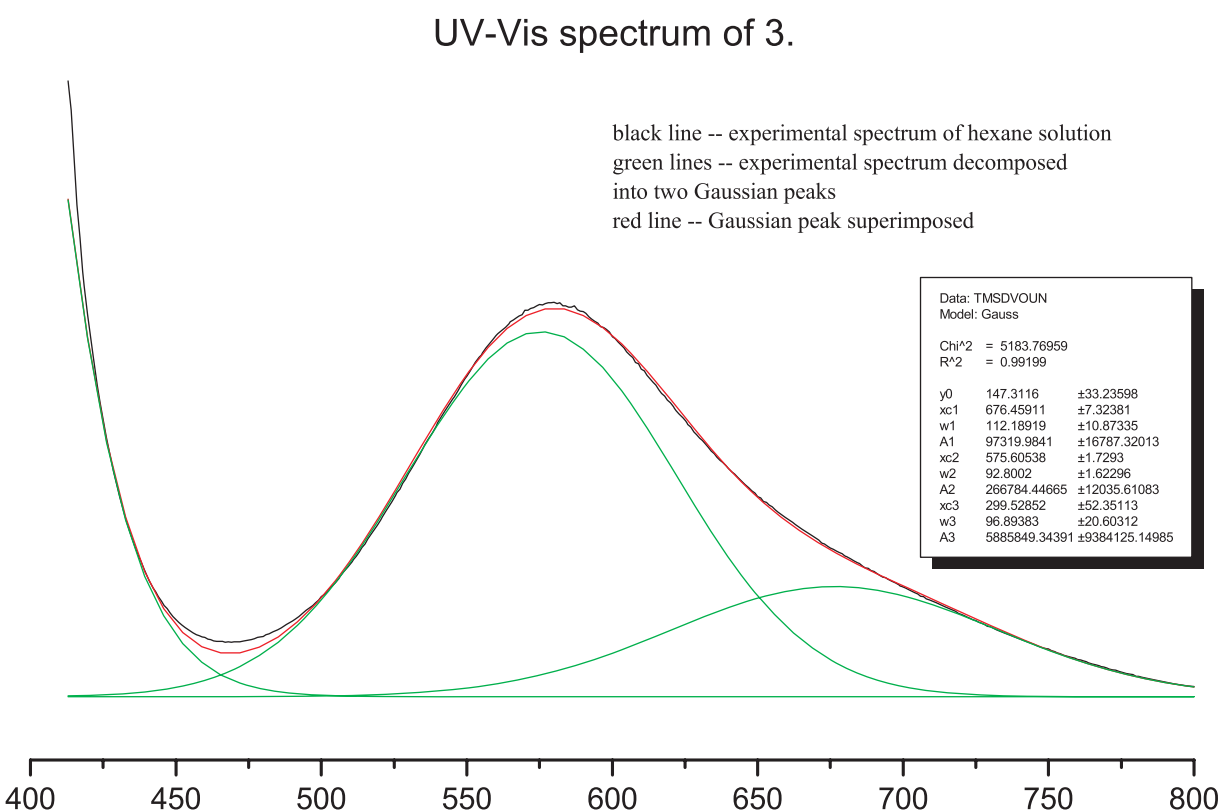

orbital drawn at 7% probability level

orbital 106

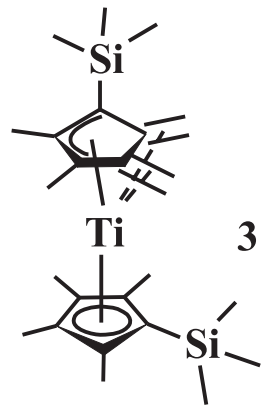

3

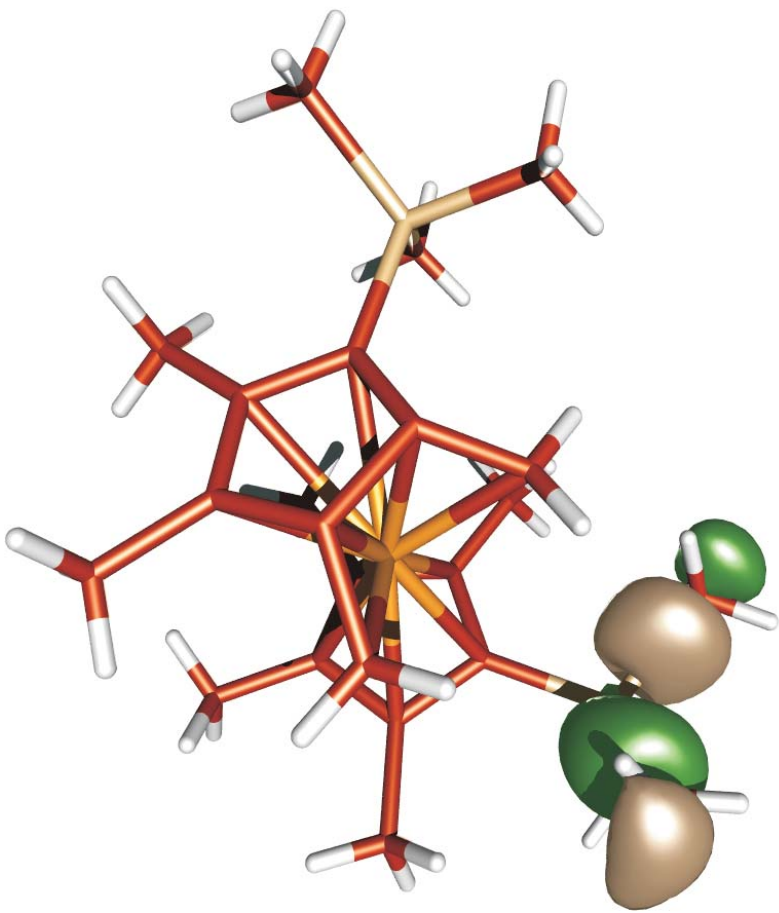

orbital drawn at 7% probability level

orbital 107

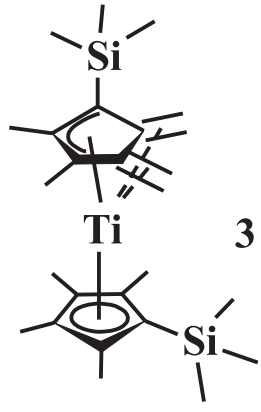

3

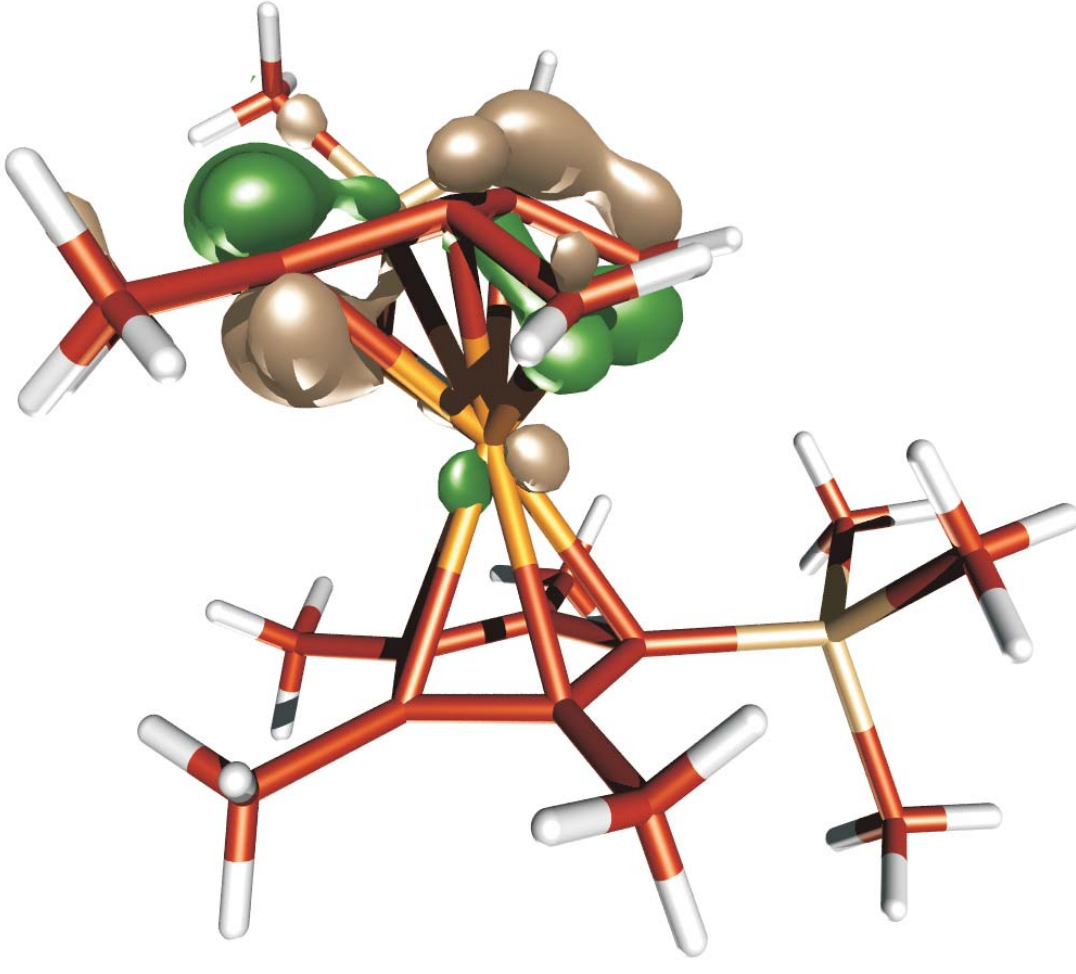

orbital drawn at 7% probability level

orbital 108

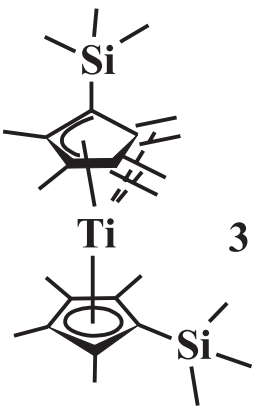

3

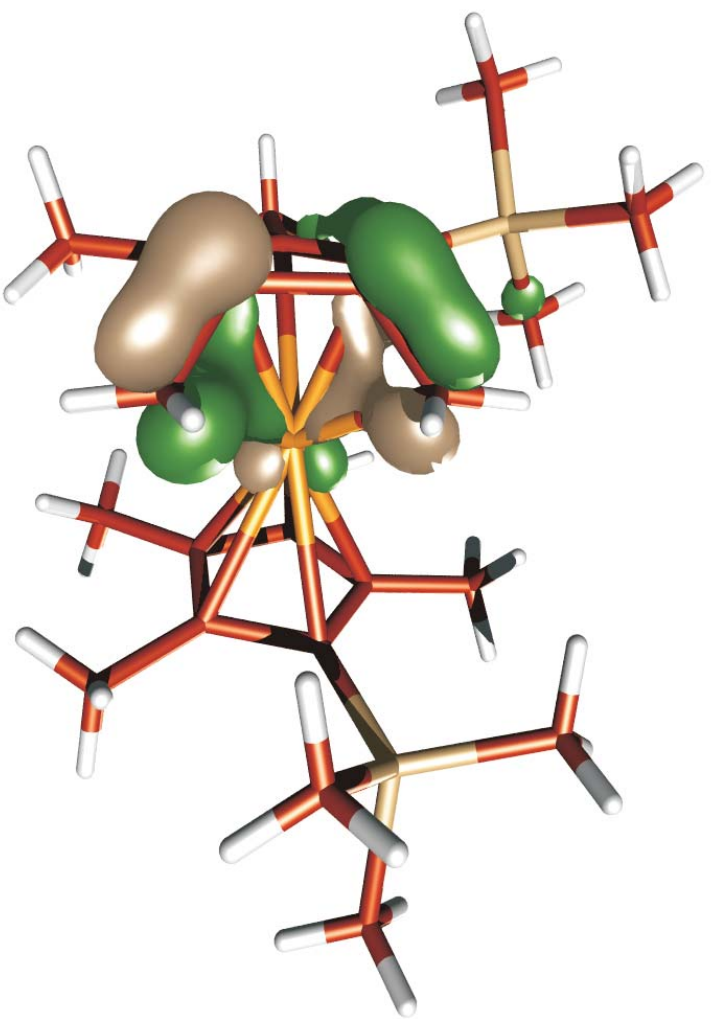

orbital drawn at 7% probability level

orbital 109

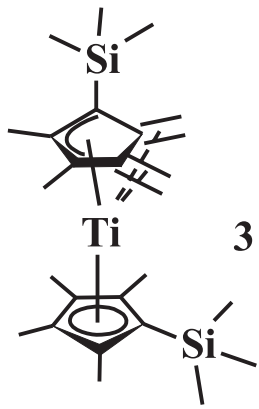

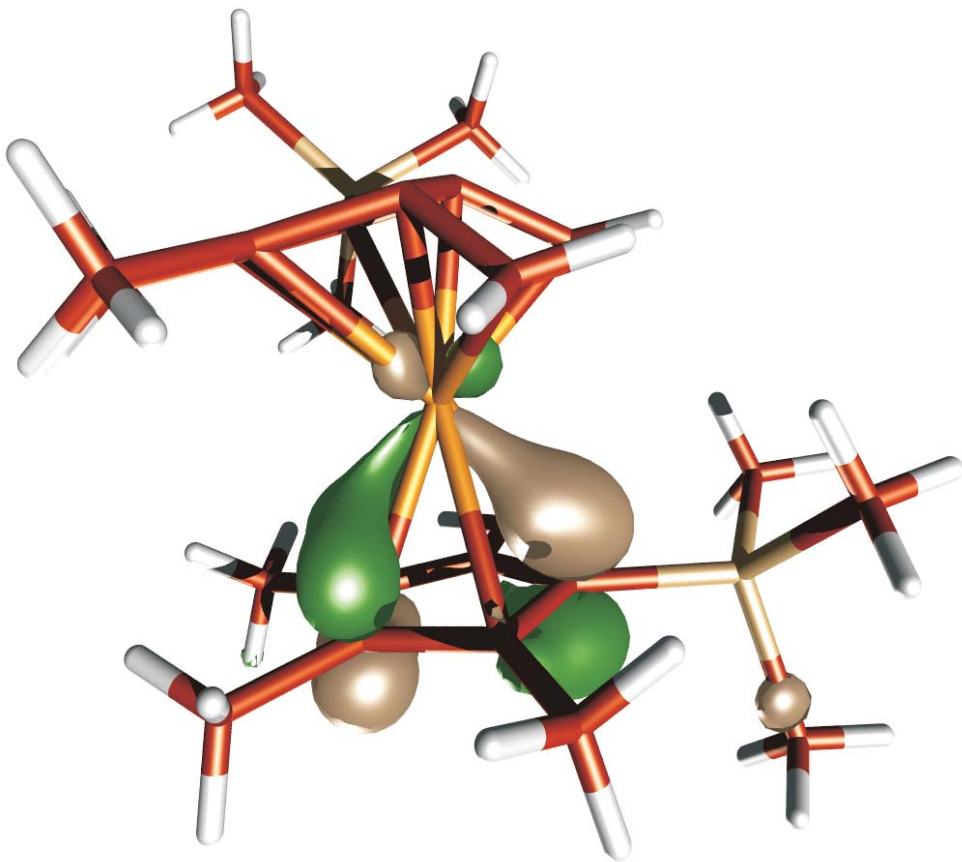

orbital drawn at 7% probability level

orbital 110

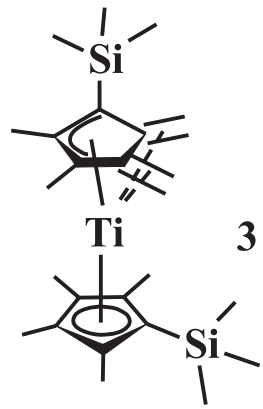

3

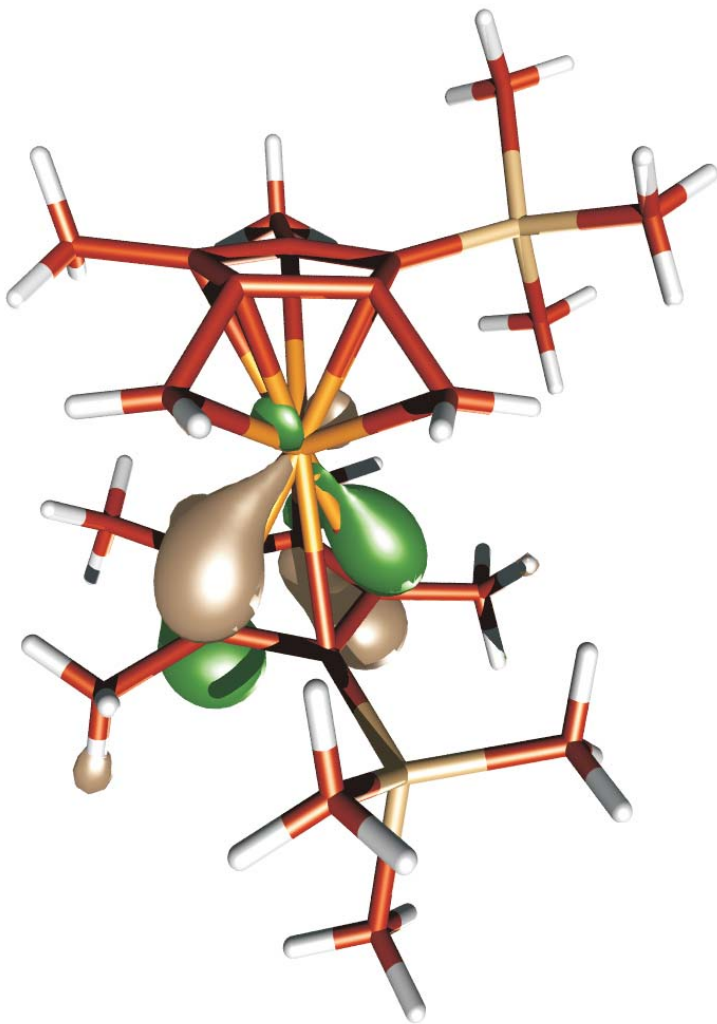

orbital drawn at 7% probability level

orbital 111

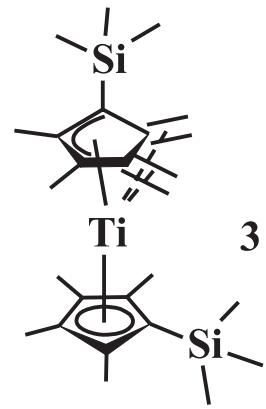

3

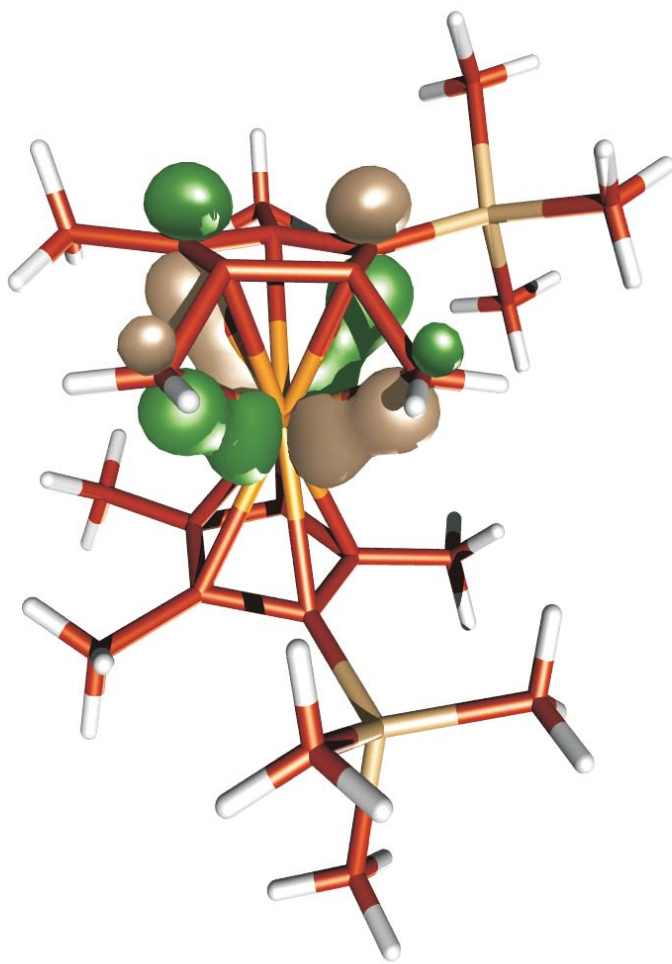

orbital drawn at 7% probability level

orbital 112 HOMO

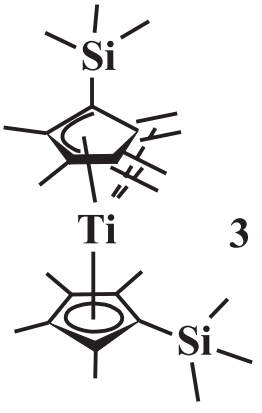

3

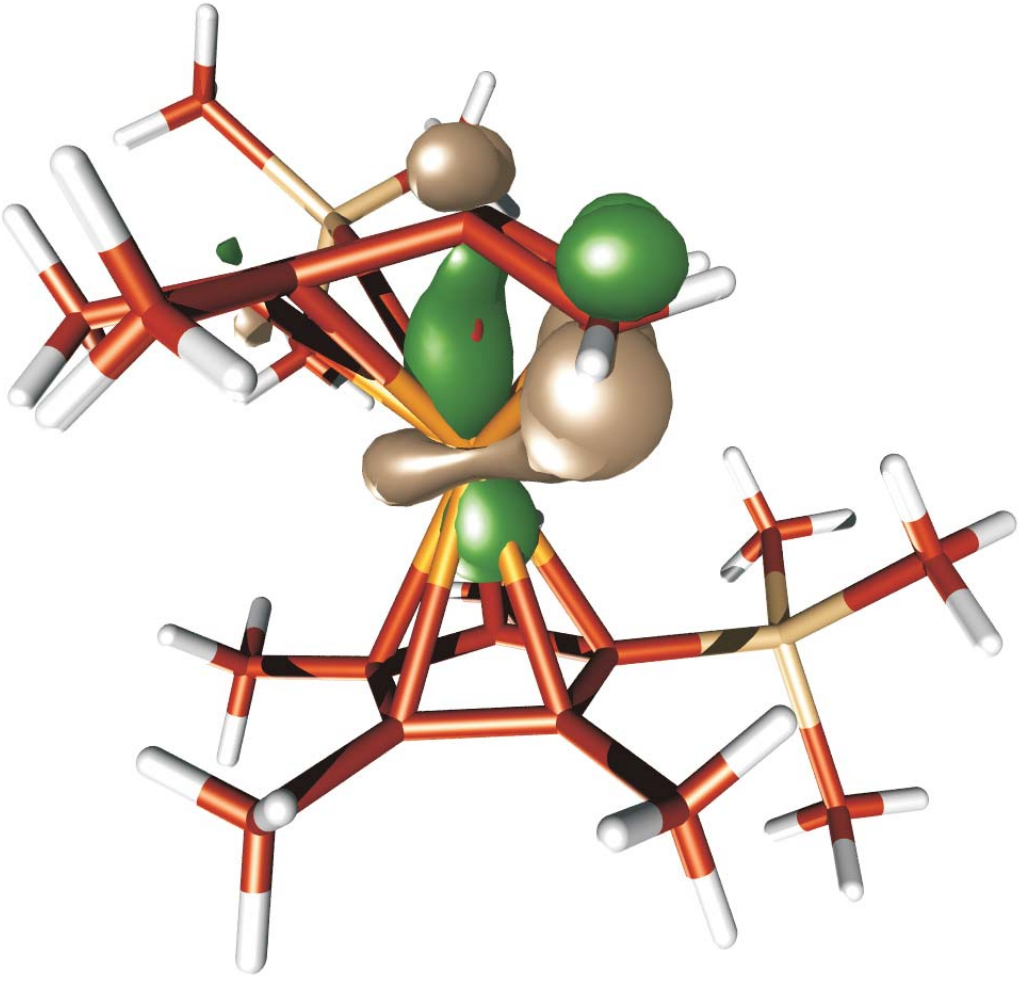

orbital drawn at 7% probability level

orbital 113 LUMO

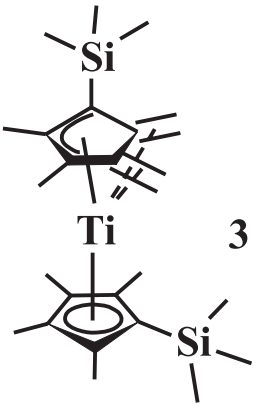

3

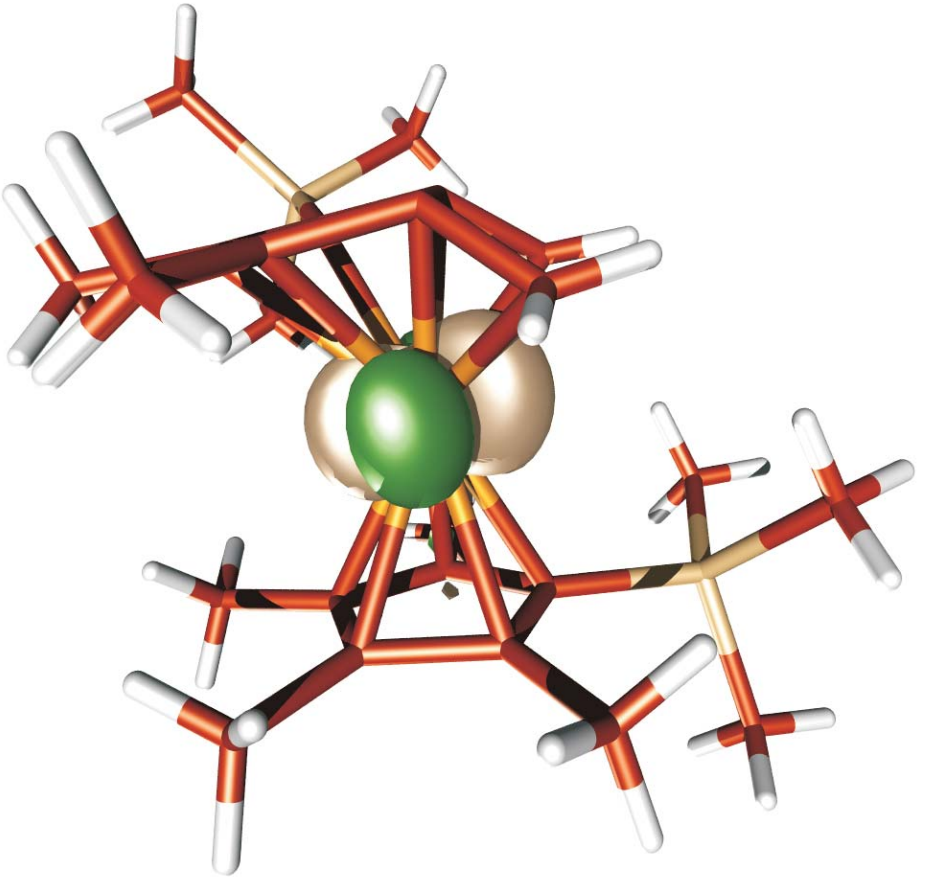

orbital drawn at 7% probability level

orbital 114

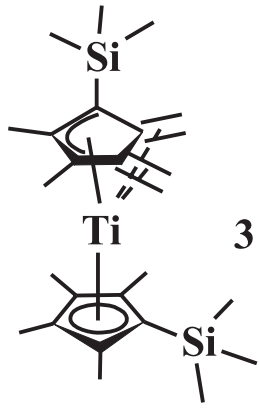

3

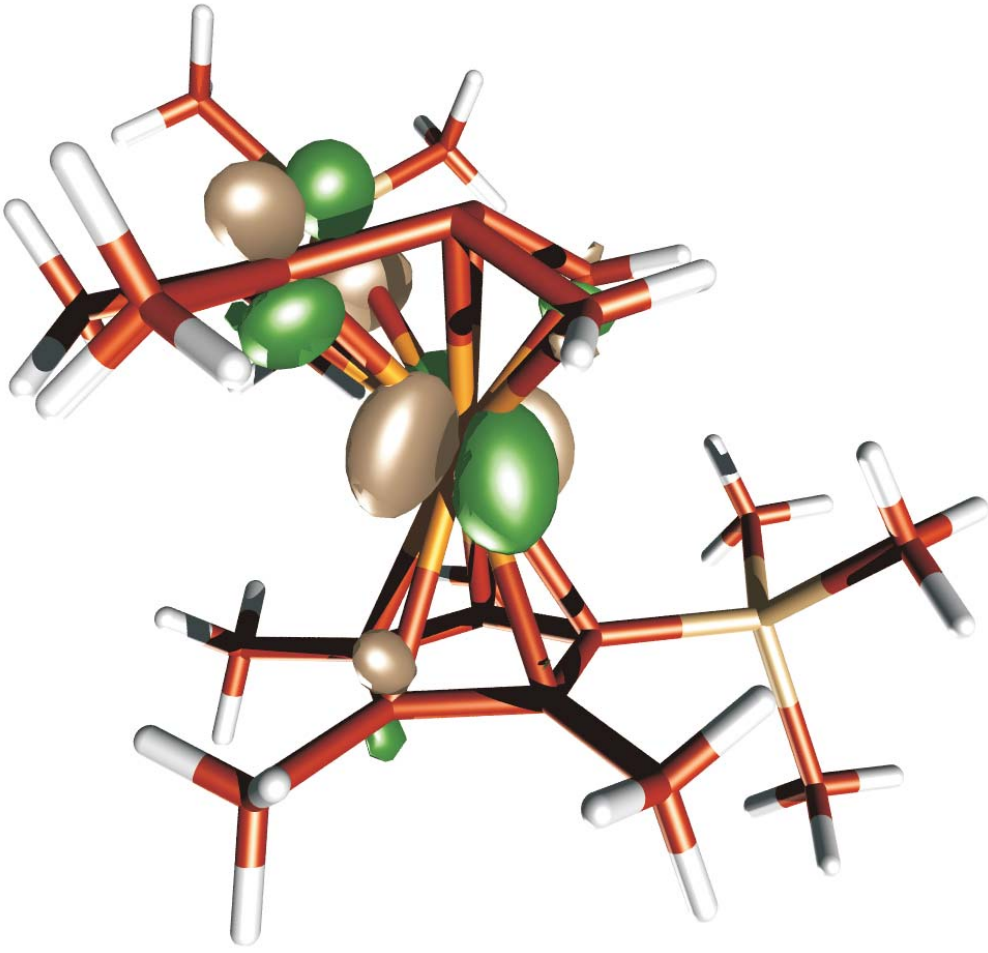

orbital drawn at 7% probability level

orbital 115

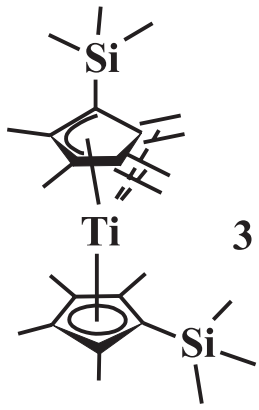

3

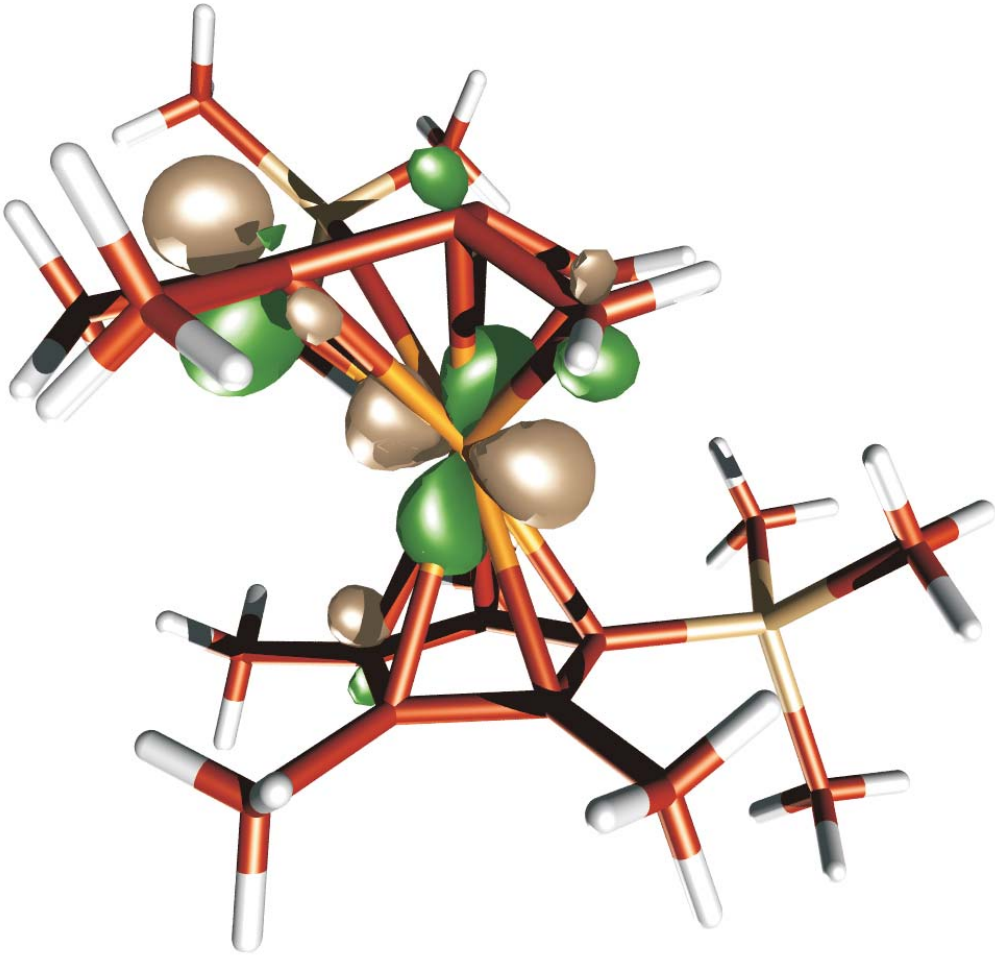

orbital drawn at 7% probability level

orbital 116

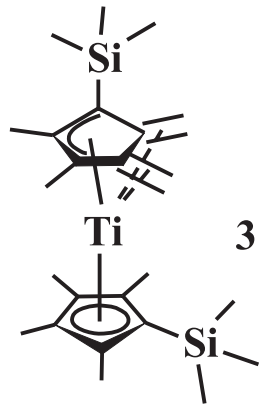

3

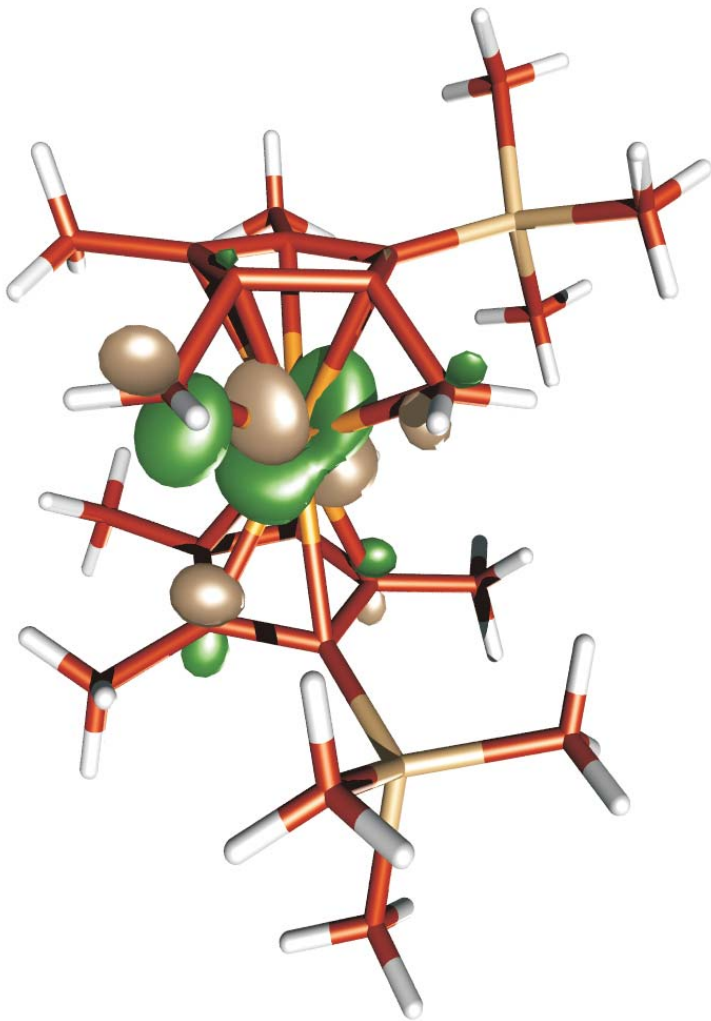

orbital drawn at 7% probability level

orbital 117

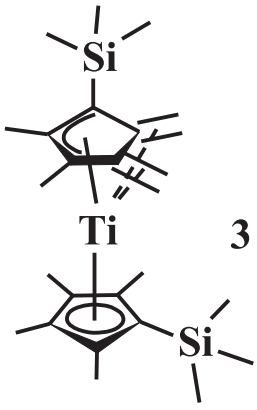

3

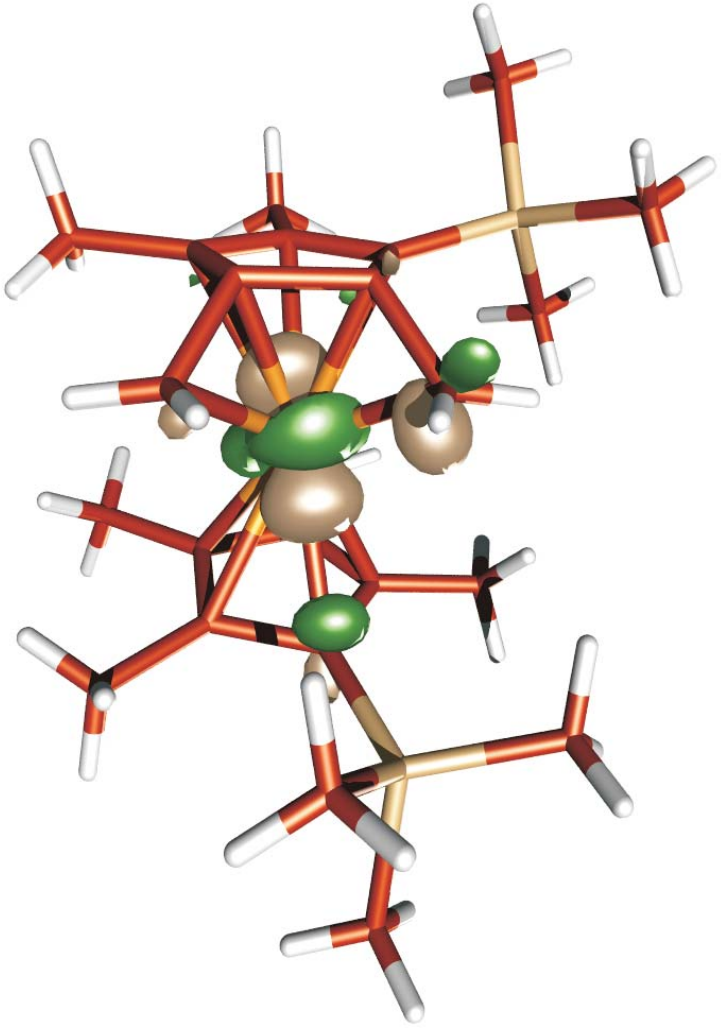

List of orbital energies for **7**

Orbital energies for **7** (in atomic units).

Orb.	Energy	
100	-0.33260	
101	-0.31355	
102	-0.30284	
103	-0.30074	
104	-0.29936	
105	-0.29012	
106	**-0.28582**	**drawn at 7% probability level**
107	**-0.26790**	**drawn at 2% and 7% probability level**
108	**-0.23068**	**drawn at 7% probability level**
109	**-0.22744**	**drawn at 7% probability level**
110	**-0.22276**	**drawn at 7% probability level**
111	**-0.20845**	**drawn at 7% probability level**
112	**-0.19096**	**drawn at 3% and 7% probability level**
113	**-0.05912**	**drawn at 7% probability level**
114	-0.02911	
115	-0.02568	
116	-0.01755	
117	-0.00683	
118	-0.00562	
119	-0.00293	
120	-0.00227	
121	0.00084	
122	0.01039	
123	0.01153	
124	0.01197	
125	0.01439	
126	0.01575	

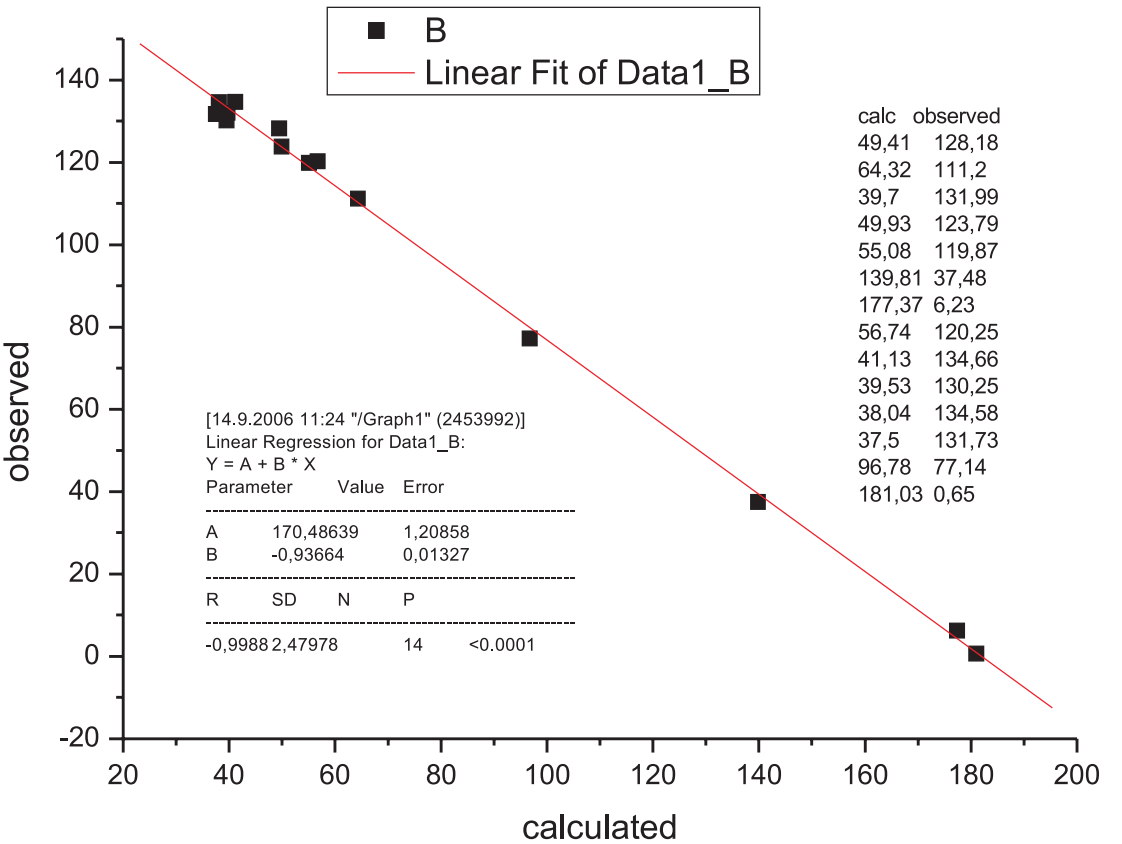

Correlation of observed ^{13}C NMR chemical shifts with GIAO ones for **7**.

orbital drawn at 7% probability level

orbital 106

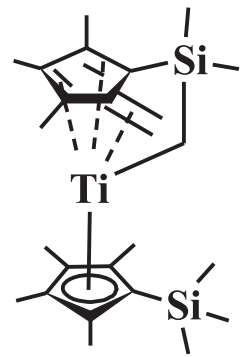

7

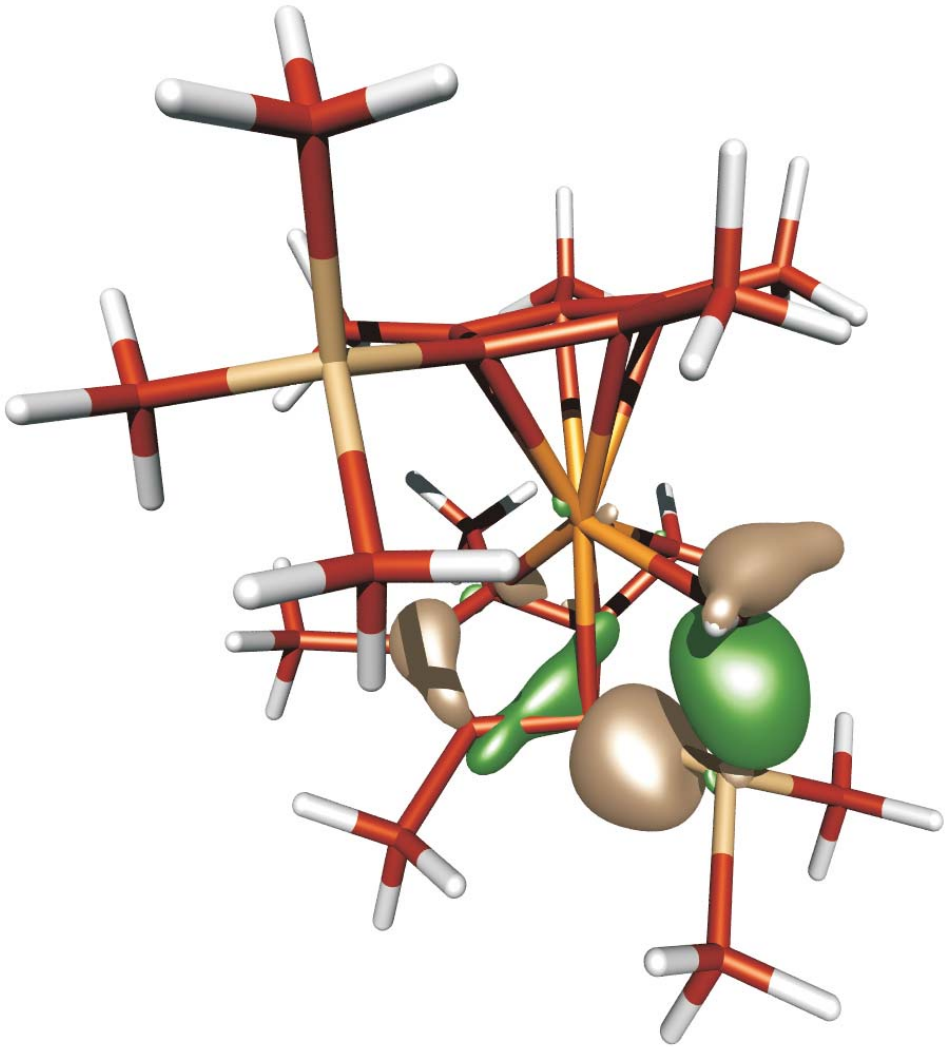

orbital 107

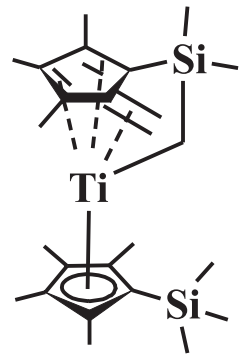

7

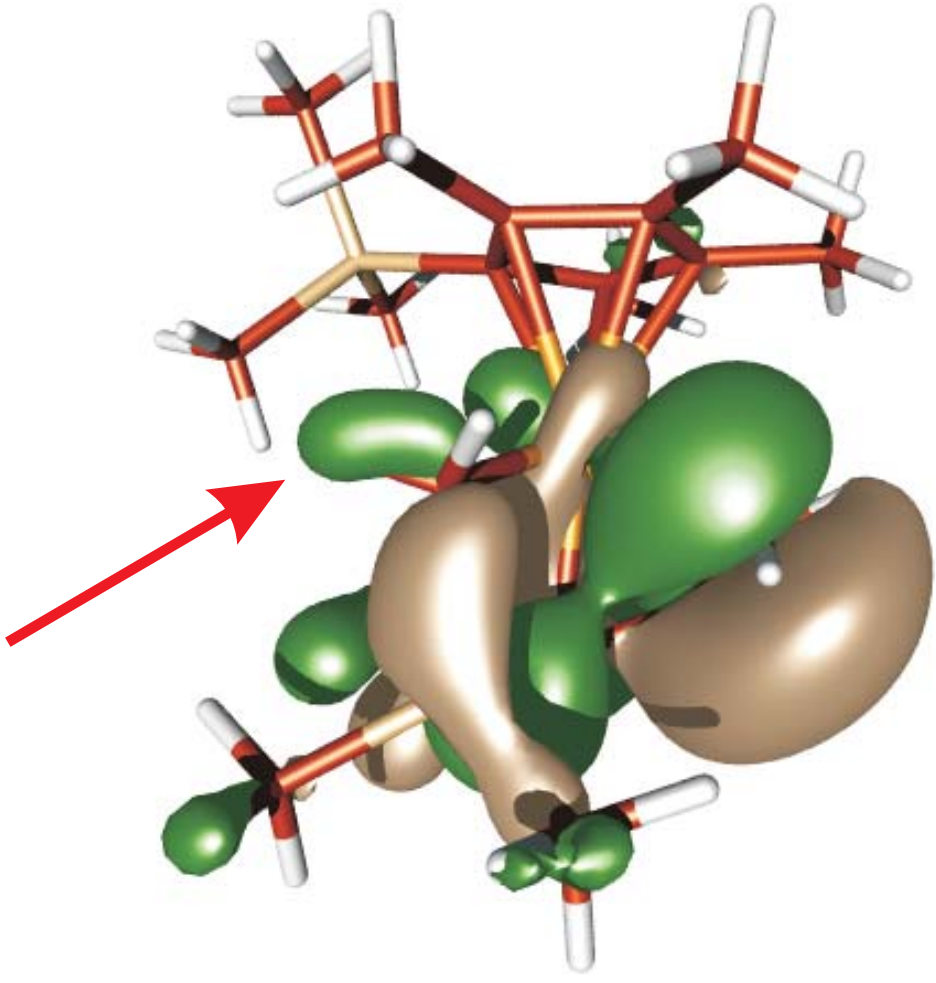

The agostic interaction occurring in the fully bonding *3c* orbital (drawn at 2% probability level) of **7.** The molecule orientation is the same as in Fig. 12.

orbital drawn at 7% probability level

orbital 107

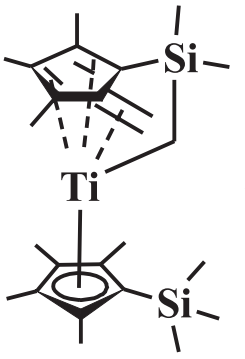

7

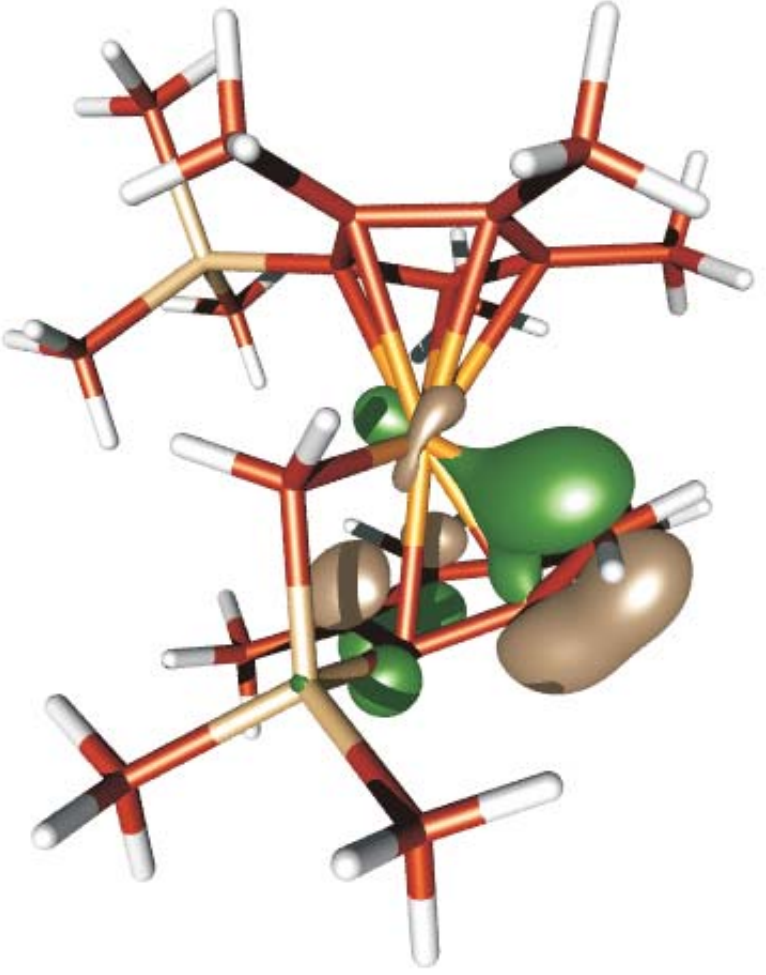

orbital drawn at 7% probability level

orbital 108

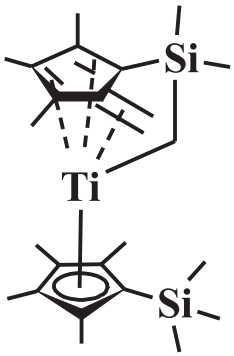

7

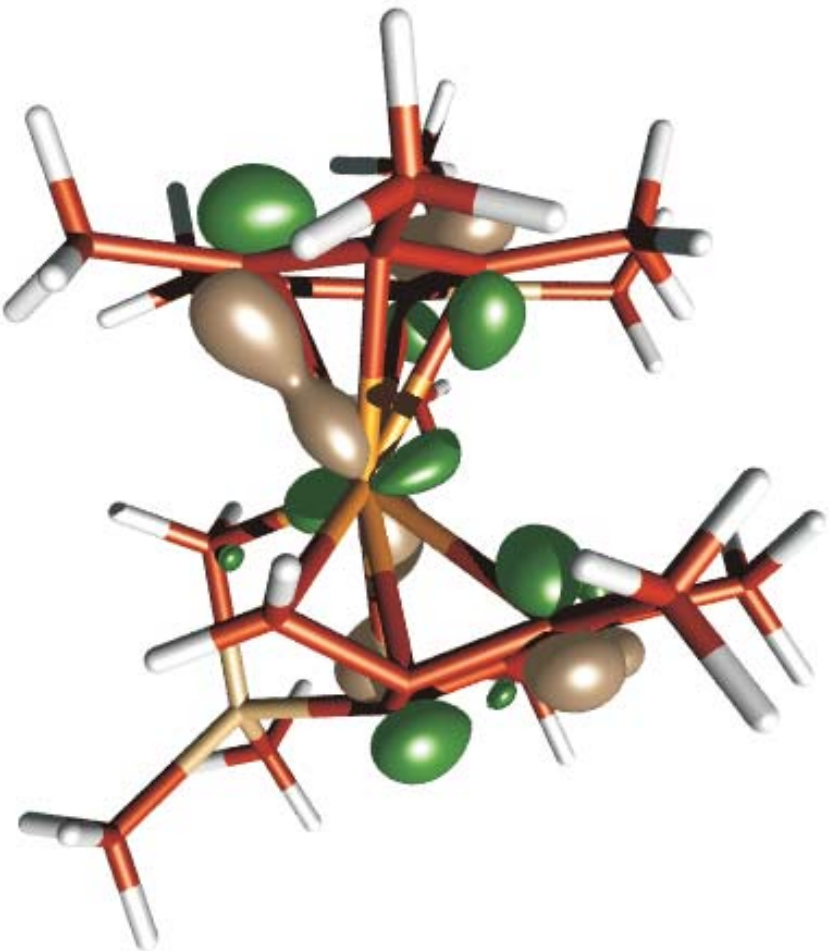

orbital drawn at 7% probability level

orbital 109

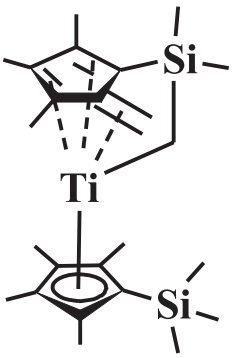

7

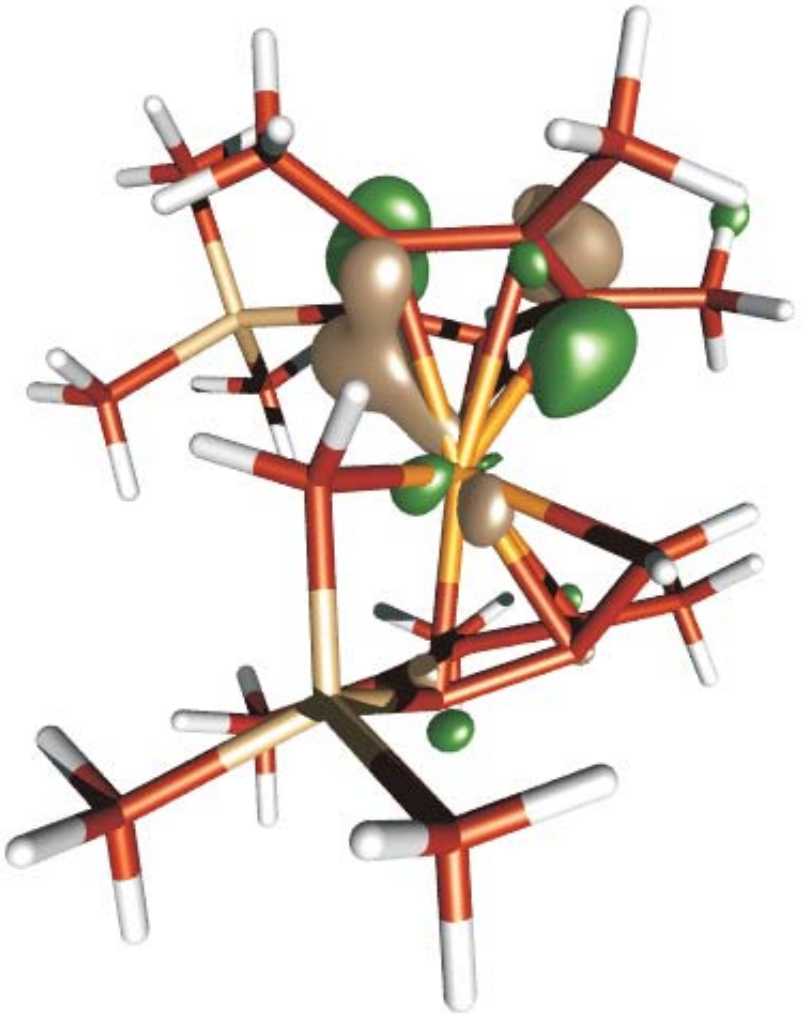

orbital drawn at 7% probability level

orbital 110

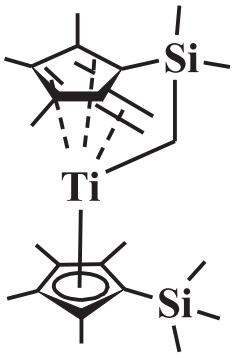

7

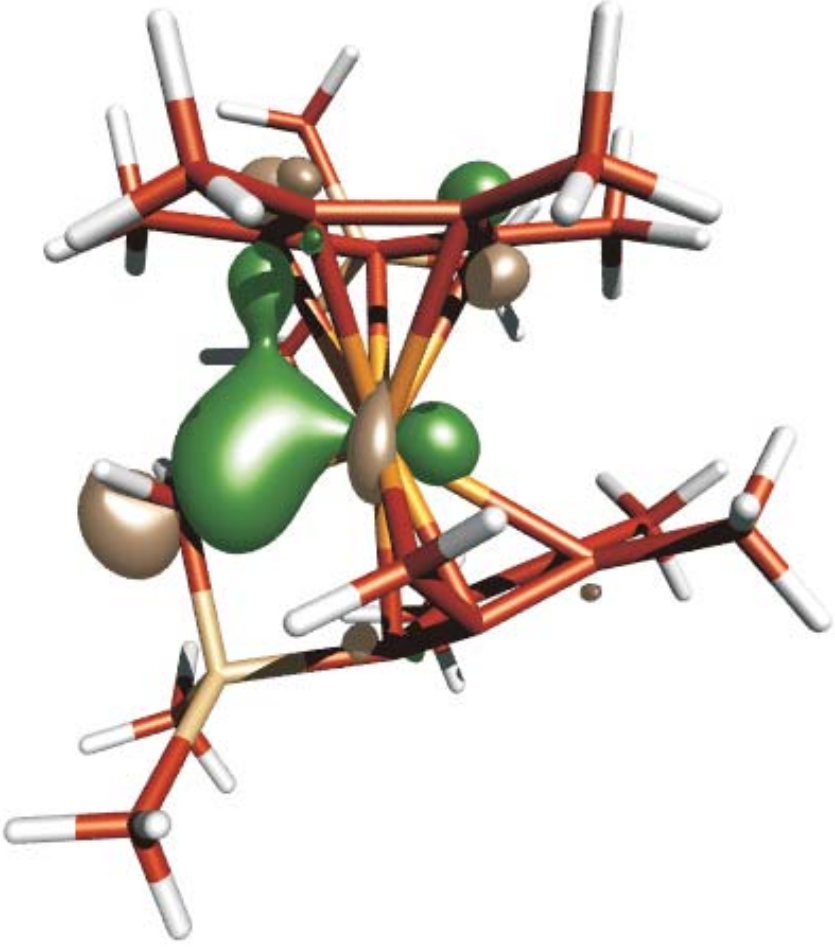

orbital drawn at 7% probability level

orbital 111

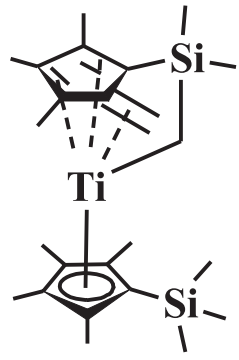

7

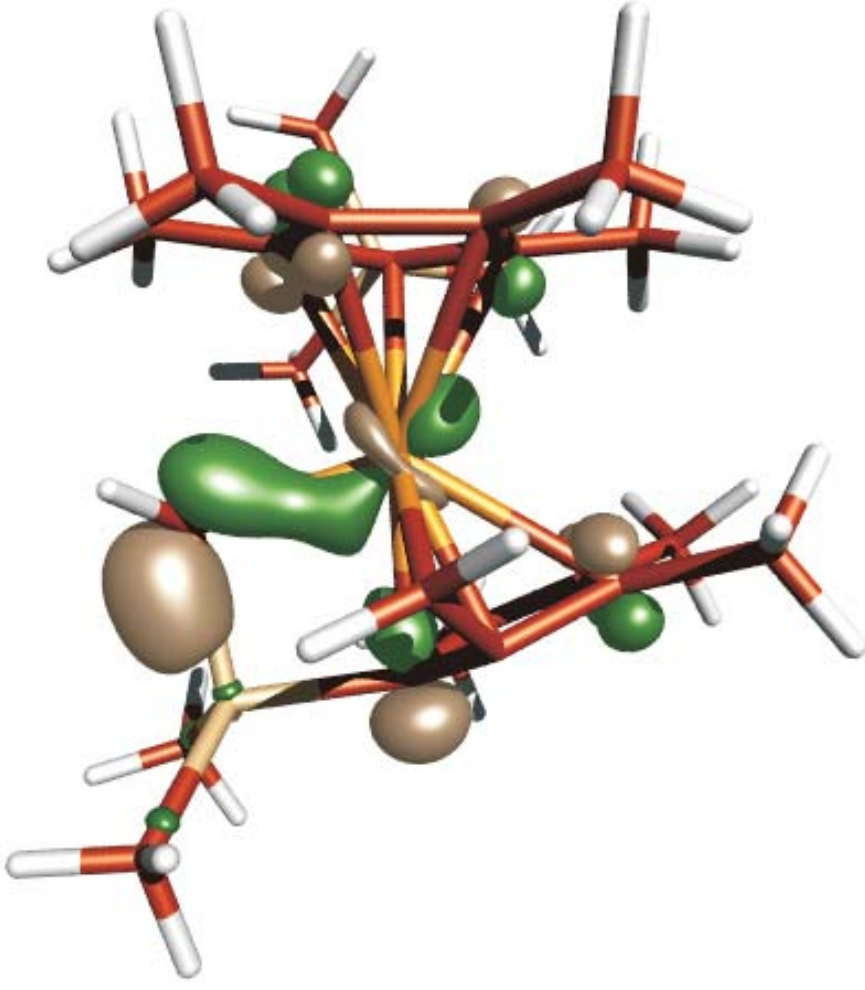

orbital 112 HOMO

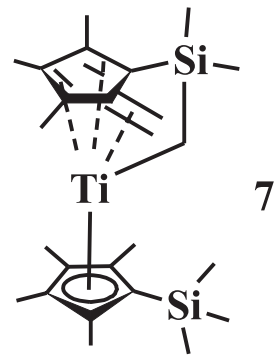

7

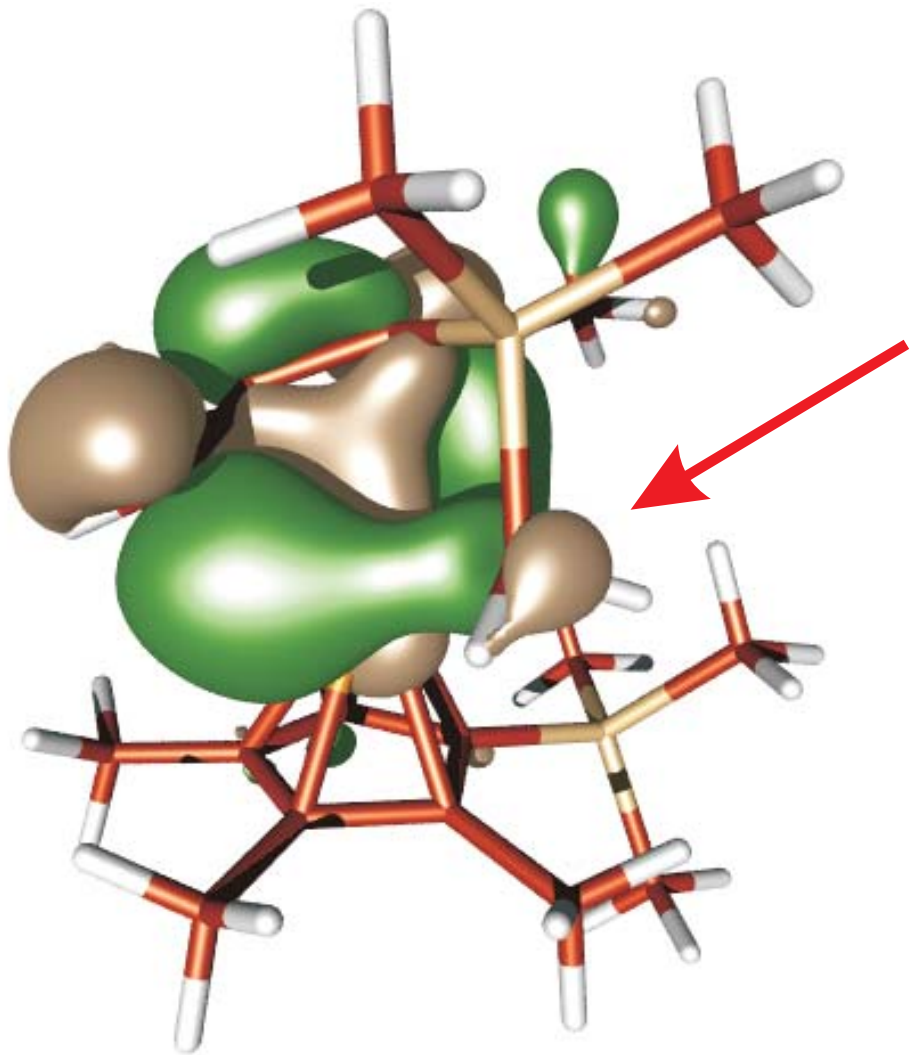

The agostic interaction occuring in the HOMO orbital (drawn at 3% probability level) of **7.** The molecule orientation is the same as in Fig. 13 .

orbital drawn at 7% probability level

orbital 112 HOMO

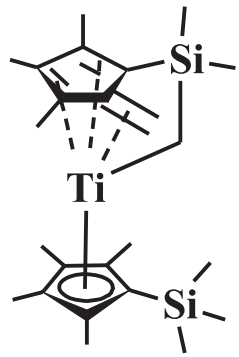

7

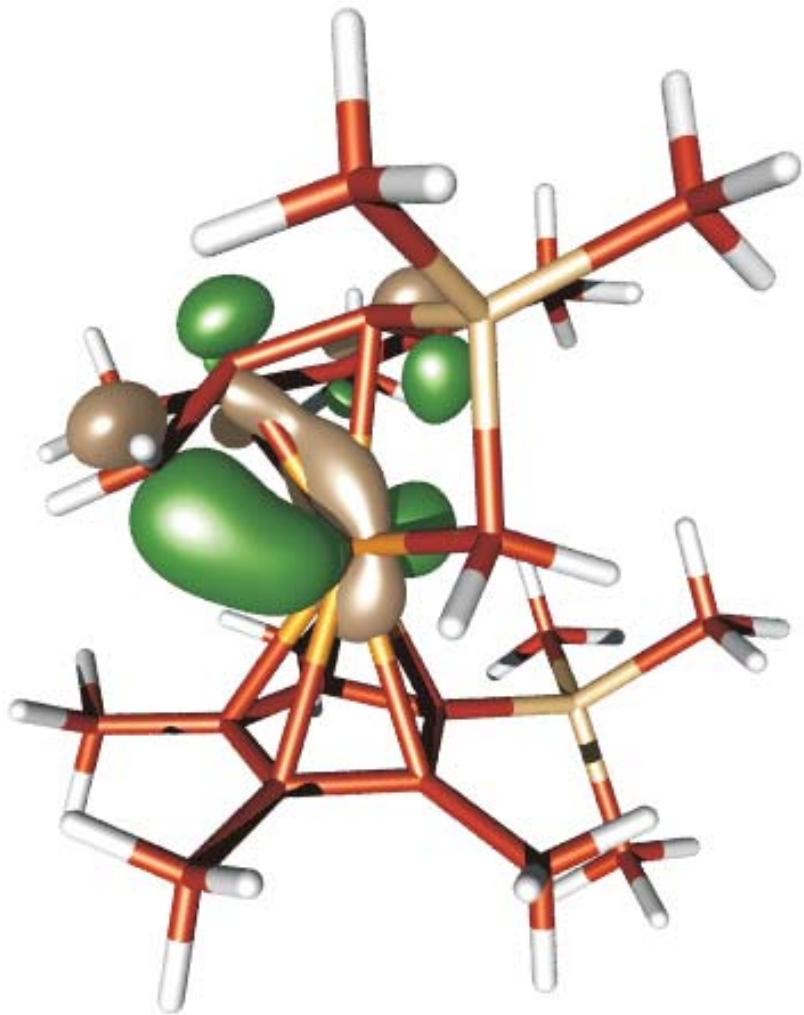

orbital drawn at 7% probability level

orbital 113 LUMO

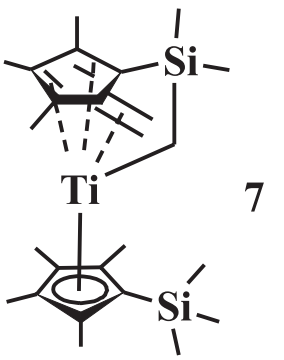

7